Journal of Advances in Radiology and Medical Imaging
Volume 4 | Issue 1
ISSN: 2456-5504

Research Article
Open Access

Comparative Simulation Study of Direct and Indirect Target Production of ^{99}Mo with Linear Accelerator at SAMEER

Aqsa Shaikh*, Dixit TS, Deshpande AP and Krishnan R

Medical Electronics Division-I, Society for Applied Microwave Electronics Engineering and Research (SAMEER), Powai, Mumbai, India

***Corresponding author:** Aqsa Shaikh, Medical Electronics Division-I, Society for Applied Microwave Electronics Engineering & Research (SAMEER), Hill Side, IIT Campus, Powai, Mumbai, India – 400076, Tel: 9664753216, E-mail: skaqsa.95@gmail.com

Citation: Aqsa Shaikh, Dixit TS, Deshpande AP, Krishnan R (2019) Comparative Simulation Study of Direct and Indirect Target Production of ^{99}Mo with Linear Accelerator at SAMEER. J Adv Radiol Med Image 4(1): 101

Received Date: March 20, 2019 **Accepted Date:** August 26, 2019 **Published Date:** August 28, 2019

Abstract

When high energy electron beam falls on a high Z target it generates bremsstrahlung photons which can be used to produce ^{99}Mo from ^{100}Mo using photo-neutron (γ, n) reaction. Two different approaches are studied to carry out photo-neutron reaction. First, a converter target approach in which photons are generated in a high Z target of tungsten using (e,γ) reaction and then (γ, n) reaction in ^{100}Mo for ^{99}Mo production. Second, a direct target approach wherein 30 MeV electrons hit directly onto ^{100}Mo target to carry out both (e, γ) and (γ, n) reactions in the ^{100}Mo target itself. GEANT4 simulation gives photons and neutrons fluxes and their angular distributions from both the approaches, which are then used to calculate activity of ^{99}Mo. The study shows that for very thin ^{100}Mo target of about 0.1 radiation length converter target shows better activity whereas, for any thickness beyond it the direct target approach is found to be more efficient. For 30 MeV and 10 kW beam falling on ^{100}Mo target with 1.4 radiation length, direct target approach is found to be more efficient. Therefore, after improvising the geometry of ^{100}Mo target in the case of direct target method an increased specific activity is obtained through GEANT4 simulation.

Keywords: Electron Linac; Activity; Bremsstrahlung; Photo-Neutrons; GEANT4; Nuclear Medicine; GDR (Giant Dipole Resonance)

Introduction

After realizing the demand of ^{99}Mo in nuclear diagnostics, various efforts are made worldwide to produce ^{99}Mo using green technology. Therefore, development of a 30 MeV high current electron linac is undertaken at SAMEER for radio-isotope production. ^{99m}Tc is a widely used radioactive tracer isotope in Nuclear Medicine. ^{99}Mo decays with a half-life of 65.976 hours to the meta-stable state of Technetium-99 (^{99m}Tc). It further decays to ground state of Technetium-99 (^{99g}Tc) by isomeric transition with a half-life of 6.0067 hours emitting a 0.1427 MeV gamma ray [1]. The emanating gamma ray energy of about 142.7 keV is convenient for detection. ^{99m}Tc, due to its short half-life, is ideal for diagnostics in nuclear imaging and 50% of total ^{99m}Tc dose is found to be excreted by the body within 1.8 days [2,3]. ^{99}Mo has a half-life of 65.976 hours which is enough to transport it as ^{99m}Tc generator to faraway locations. These advantages have accelerated the extensive use of ^{99m}Tc in medical scans. Today production of ^{99}Mo depends entirely on reactor-based technology using Highly Enriched Uranium (HEU) [4]. There are five reactors in the world HFR (High Flux Reactor) in Netherlands, BR-2 (Belgian Reactor) in Belgium, NRU (National Research Universal) reactor in Canada, OSIRIS in France, SAFARI-1 (South Africa Fundamental Atomic Research Installation) in South Africa where preparation of ^{99}Mo is usually done. Out of these NRU, Canada has been permanently shut down in March, 2018 creating huge difference in demand to supply ratio of ^{99}Mo [5]. HFR and BR-2 are expected to expire in 2024 and 2026 respectively [6]. This will give rise to differences in demand to supply ratio of ^{99}Mo. In India, there are almost 280 nuclear imaging facilities operational as of 2018 based on AERB (Atomic Energy Regulatory Board) data. ^{99}Mo generators are supplied from BRIT (Board of Radiation & Ion Technology) and also from other countries like Israel, Turkey, and UK etc. The strength of the generator decides the cost, which can vary from INR 27,000 to INR 70,000. Treatment cost depends on the dose administered to the patients, which can range from 2 mCi to 20 mCi depending on the type of scan. Today, over 70% of nuclear medical procedures include the use of ^{99m}Tc [7]. Due to its wide use in nuclear medicine, it is important to find environment friendly and cost effective ways to produce ^{99}Mo [8]. Apart from neutron induced fission of ^{235}U, various other reaction channels using neutrons, protons, electrons/photons are possible to produce ^{99}Mo or ^{99m}Tc directly when they are bombarded on ^{235}U, ^{238}U, ^{98}Mo and ^{100}Mo targets [9-11]. One of the reaction channels is ^{98}Mo (n,γ) ^{99}Mo, where thermal and epithermal neutrons provide highest reaction cross-section but still few hundred times lesser than the thermal neutron induced fission reaction cross-section of ^{235}U. Proposals for ^{98}Mo (n, γ) ^{99}Mo reaction include the use ADSR (Accelerator Driven Sub critical Reactors) to carry out neutron capture or fission of ^{98}Mo or ^{235}U, respectively [12]. Another reaction channel is ^{100}Mo (p, 2n) ^{99m}Tc, which produces ^{99m}Tc directly but due to the short half-life of ^{99m}Tc it has to be produced and utilized locally. There are also proposals of using electron accelerator to produce ^{99}Mo by means of photo-neutron reaction of ^{100}Mo. T. Ruth in his report proposed the use of accelerators as one of the most effective future ideas for producing ^{99}Mo [13]. The photons required for ^{100}Mo to ^{99}Mo conversion can be obtained from electron accelerators as bremsstrahlung photons. This is expected to give higher specific activity than neutron capture of ^{98}Mo [10]. According to various references and studies carried out for production of ^{99}Mo, specific activity of ^{99}Mo is found to vary depending upon method of production and target used [14-16]. Currently, Canadian Isotope Innovations Corporation's (CIIC's) has proposed the use of linac for the production of ^{99}Mo via $^{100}Mo(\gamma,n)^{99}Mo$ reaction to produce about 1,100 Ci/week of ^{99}Mo. NorthStar, Wisconsin, is also looking forward to produce ^{99}Mo through photo-neutron reaction and is expected to bring the technology in the market by the end of 2019 [17]. In a patent published by Diamond *et al*. the electron linac based technology for producing ^{99}Mo has been studied thoroughly [18].

At SAMEER, looking at various efforts made worldwide to produce ^{99}Mo using green technology, a project to study accelerator based production of ^{99}Mo using 30 MeV high beam power electron linac is undertaken. A prototype of the 30 MeV electron linac is to be developed in two stages. In first stage, a 15 MeV 3-5 kW linac will be developed followed by an upgraded 30 MeV-10 kW beam power linac. ^{99}Mo will be produced via photo neutron reaction using enrich ^{100}Mo target. Cross-section of (γ, n) reaction peaks at photon energy 14-15 MeV up to 0.15 barns. 30 MeV electron linac is expected to produce enough photon flux of energies up to 30 MeV which is used for ^{99}Mo production through ^{100}Mo (γ, n) ^{99}Mo reaction. In this paper, first SAMEER linac parameters are described and in section II, GEANT4 simulations for beam energy optimization is explained. Later, section III describes direct and indirect target approaches with target optimization and activity calculations.

Methods and Materials

SAMEER has designed, developed and successfully tested side coupled; standing wave structure operating at π/2 mode with an operation frequency of ~ 3 GHz. Linac with 15 MeV energy is successfully tested as a prototype development [19]. Therefore, to achieve 30 MeV, two 15 MeV linacs in series operation is proposed. Schematic of the layout is shown in Figure 1. The main parameters of the linac are given in Table 1.

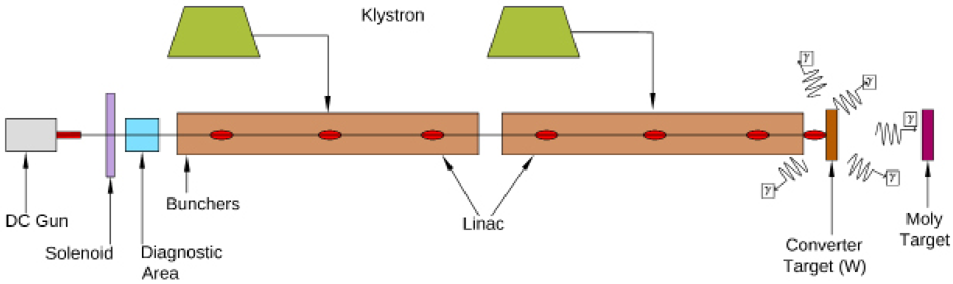

Figure 1: Schematic diagram of 30 MeV electron linac layouts

Parameters, Unit	Value
Energy, MeV	30
I_{ave}, μA	350
Duty cycle	0.00514
I_{peak}, mA	68
P_{beam}, kW	10.5
Pulse width, μs	12.85
Rep rate, Hz	400

Table 1: Linac Parameters

In the proposed design, a 60 kV DC triode gun is the source of electrons with pulse mode operation followed by diagnostic area for current and emittance measurement. First linac is comprised of 3 and ½ buncher cavities and remaining cavities are fixed length accelerating cavities. Second linac is comprised of only fixed length accelerating cavities. Two independent klystrons provide RF power to the linac and they are synched by a master signal from the RF driver's control unit. Exit end of the second linac is connected to a very thin (150 μm) low atomic number (Z) material window. Electrons after gaining 30 MeV energy falls on a high Z material target like tungsten and produce bremsstrahlung radiation in all directions. Photons in the forward direction are collimated and fall on enriched molybdenum target for (γ, n) reaction. A very high duty operation of linac is expected to get the desired beam power. The target used is retractable type, wherein low and high Z target is inserted in the beam path for bremsstrahlung generation or for beam dump. One more port with low Z material window is designed for direct irradiation of Mo targets. The targets are water cooled and thermal design is done using ANSYS software [20].

GEANT4 Simulations

GEANT4 (Geometry and Tracking) simulating tool is used to design the target and estimate ^{99}Mo activity [21]. It is a Monte-Carlo based simulation tool which takes source particles as individual events. Simulations with 20 million events are found to be statistically sufficient without loading the computer processor and RAM. A 30 MeV pencil electron beam source and W/^{99}Mo targets surrounded by detectors are kept in a box of vacuum for GEANT4 simulations. A simplistic spherical photon and neutron detector is designed to find out photon and neutron fluxes as well as their angular distributions. Validation of the GEANT4 code is done using standard data available in references and experimental results from SAMEER's 6 MeV linac. The reaction under study is the $^{100}Mo(\gamma,n)^{99}Mo$ reaction, where photons and neutrons are used in estimating the production of ^{99}Mo. Hence, the most important data for validation is of photon flux and neutron flux generated by the code. In Figure 2 a photon flux angular distribution graph from Berger-Seltzer is reproduced using the initial parameters mentioned in the reference [22].

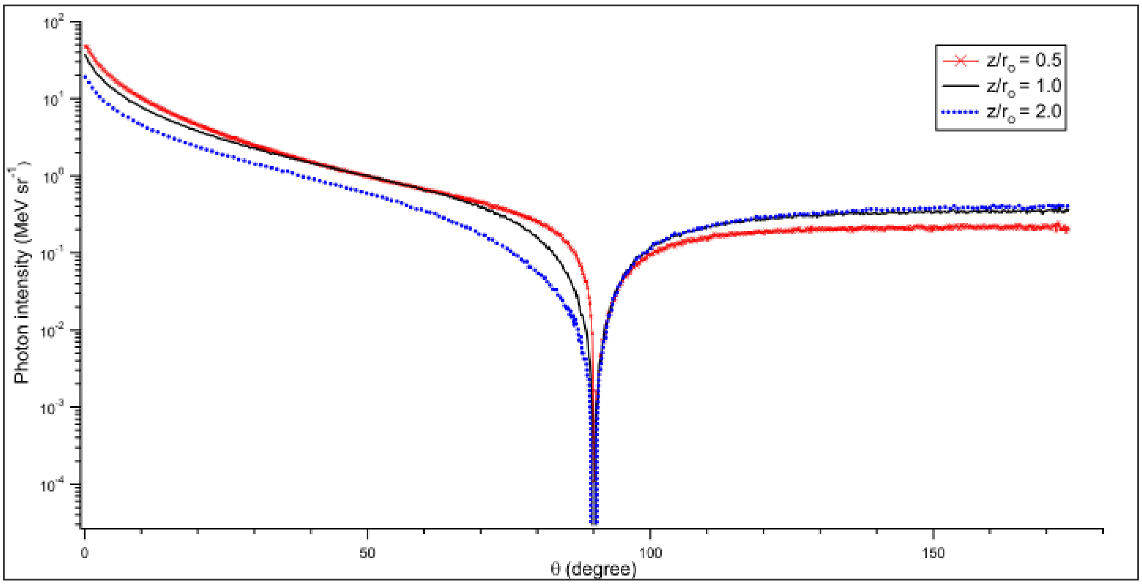

Figure 2: Angular distribution pattern of photon flux obtained from tungsten target of thicknesses 0.5, 1.0 and 2.0 radiation length and infinite length perpendicular to the electron beam of energy 30 MeV

The graph shows similar pattern to the reference graph. It has a strong forward direction peak and sharp dip at 90° angle from beam direction. This dip is observed due to practically infinite target thickness in X and Y plane whereas the beam is incident in Z direction. The forward direction peak obtained from GEANT4 is slightly lower than what is given in the reference and a difference of 11.80%, 13.40% and 9.03% is observed for tungsten target of thickness 0.5, 1.0 and 2.0 r.l. respectively. This discrepancy matches with the mentioned difference of up to 25% for angular distribution maxima in forward direction due to normalization between experimental and computed data [23]. GEANT4 simulation data is also compared with an experimental result from SAMEER's 6 MeV electron linac. This comparison is shown in Figure 3.

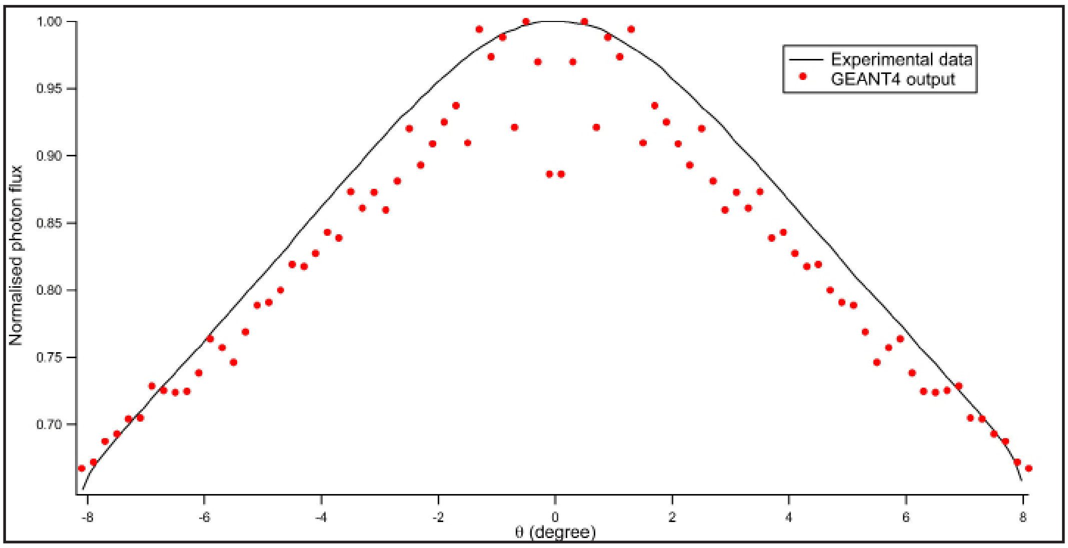

Figure 3: Comparison of experimentally and GEANT4 simulation based normalized photon flux angular distribution for 6 MeV electron linac on 1.5 mm thick tungsten and copper backing of 2.5 mm

During experiment 6 MeV electron beam is bombarded on a 1.5 mm thick tungsten target with 2.5 mm thick copper backing. The photon beam is collimated in a small angle of 12 °. The measurement is done on Radiation Field Analyzer (RFA). The plot shows less than 10% difference between experimental values and GEANT4 data in Figure 3. Similarly, validation of neutron flux data is done by comparing values given in reference paper of Barber and George [24]. For the given initial condition of 1 radiation length (r.l.) of ^{100}Mo target and 34.3 MeV electron beam energy, neutron flux coming out of ^{100}Mo using GEANT4 is 10.7315x10^{-4} n/e which is comparable with the interpolated value of 12x10^{-4} n/e [24].

Beam Energy Optimization

Bremsstrahlung photons coming from (e, γ) reaction in a high Z target is used to carry out ^{100}Mo(γ,n)^{99}Mo reaction. The bremsstrahlung photons are of continuous energies starting from 0 up to electron beam energy. Depending upon the required energy of photons, first, optimization of electron beam energy of the linac is done. Tungsten (Z=74) is considered as electron to photon converter target. Bremsstrahlung flux spectra are obtained as given in Figure 4 with energy variation of electron beam energy.

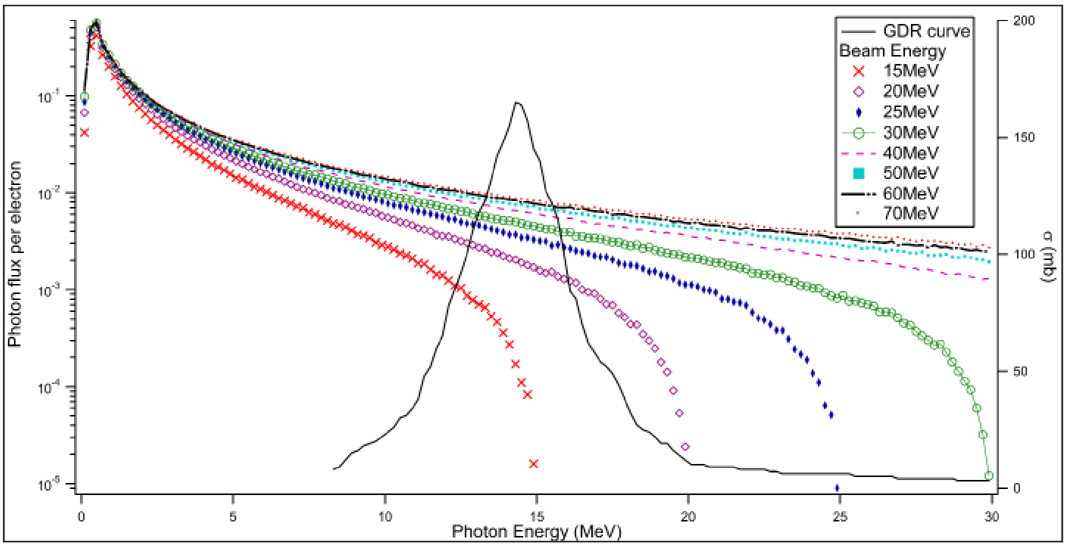

Figure 4: Plot of photon flux (Y-axis-left) and ^{100}Mo (γ, n) ^{99}Mo reaction cross-section (Y-axis-right) vs. photon energy. The GDR curve is associated with Y-axis on right hand side showing microscopic reaction cross-section in mb for ^{100}Mo (γ, n) ^{99}Mo reaction. Bremsstrahlung photon flux intensity per electron for various electron beam energy incident upon tungsten target of 0.8 radiation length is plotted along with GDR curve

As seen in Figure 4, when one increases the electron beam energy from 15 MeV to 70 MeV, the total photon flux and the end point energy of bremsstrahlung increases, which is expected from a typical bremsstrahlung pattern. But it is also observed that increasing electron beam energy does not appreciably increase the number of effective bremsstrahlung photons (12-17 MeV) under the GDR curve and mostly the photon flux of higher energy increases. Hence, a 30 MeV electron beam seems reasonable for the production of ^{99}Mo by ^{100}Mo (γ, n) ^{99}Mo reaction. Further increase in the energy of electron will provide more number of photons of higher energy that can lead to production of other isotopes by (γ, 2n) (γ, 3n) and (γ, pn) reactions [25].

Method of Production

After deciding on electron beam energy and validating GEANT4 codes, two approaches to carry out ^{100}Mo (γ,n)^{99}Mo reaction are studied as shown in Figure 5.

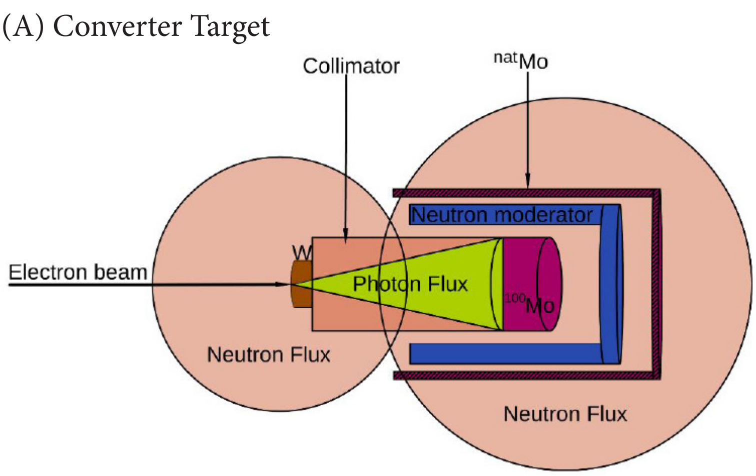

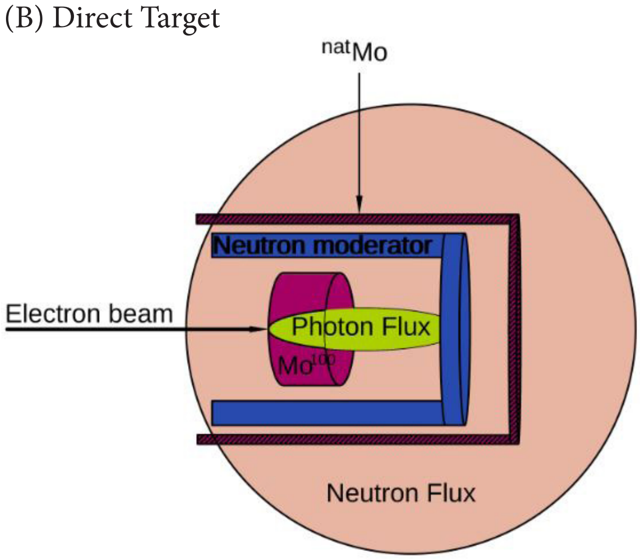

Figure 5: Schematic diagram of two methods of production of ^{99}Mo using 30 MeV electron linac **(A)** Shows the converter target method where tungsten is used as electron to photon converter and then hitting those photons on ^{100}Mo, whereas **(B)** shows direct target method for the production and utilization of photons in the ^{100}Mo target itself

A) Converter target approach: In this approach, a converter target is kept before Mo target to produce photon flux required for ^{100}Mo(γ,n) ^{99}Mo reaction. Tungsten being high Z material and high melting point is suitable for electron to photon conversion.

B) Direct Target approach: In this approach, electron beam hit directly on to ^{100}Mo target. Mo target has sufficient bremsstrahlung conversion efficiency because of its relatively high atomic number, Z=42. It is expected that the bremsstrahlung photons produced locally are utilized at the same ^{100}Mo target to give ^{99}Mo.

Converter Target Approach

Target Thickness Optimization

After beam energy optimization, geometry of converter target is optimized. The optimization is done to obtain maximum effective photon flux. Using GEANT4, thickness of tungsten is varied between 0.1 and 5 r.l. and plotted along with GDR curve obtained from Beil H, *et al.* see Figure 6.

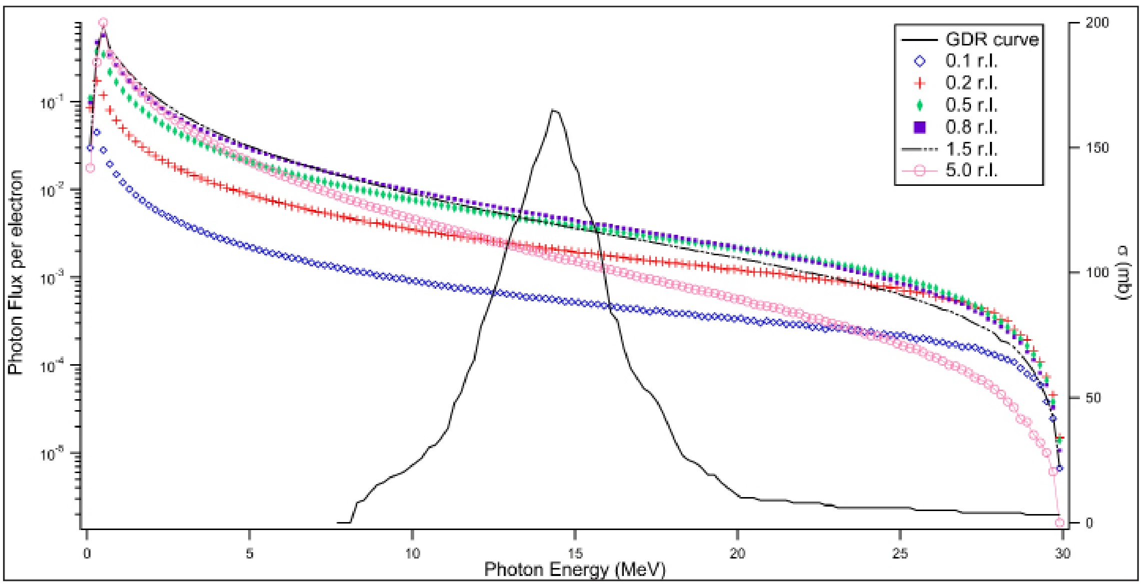

Figure 6: The GDR curve is associated with Y-axis on right hand side showing microscopic reaction cross-section (σ) in mb for ^{100}Mo(γ,n) ^{99}Mo reaction. Bremsstrahlung photon flux intensity per electron for various target thickness starting from 0.1 to 5.0 radiation length is plotted with GDR curve

The thickness of target at which maximum area under the GDR curve is obtained is best suited for electron photon conversion. It is observed that for very thin targets many electrons come out of the target without interacting completely thus producing less photon flux. As target thickness increases, photon flux also increases but soon saturates after few r.l. thick targets. When thickness is increased to 1.5 r.l. the effective photon flux is found to have decreased in the region of GDR curve and for 5 r.l. the photon flux under GDR curve is further reduced. This happens because of self-absorption of photons inside tungsten target. Hence increasing the thickness of target beyond a particular value is found to decrease the photon flux. An optimized thickness of converter target is one where there is maximum electron interaction and minimum self absorption. For further optimization, flux weighted average reaction cross-section (σ_a) is calculated for various thickness of tungsten [26]. σ_a gives reaction cross section weighted over photon flux and directly relates photon flux generation to ^{99}Mo production probability. Flux weighted average reaction cross-section is given by following equation-

$$\sigma_a = \frac{\sum \varphi(E)\sigma(E)}{\sum \varphi_{(E>8.2MeV)}} \quad (1)$$

In Figure 7 Thickness of tungsten target is plotted against flux weighted average reaction cross- section (σ_a) for ^{100}Mo(γ,n)^{99}Mo reaction. Maximum reaction cross-section is obtained for tungsten target of thickness 0.8 r.l. Hence, tungsten of 0.8 r.l. thickness is decided to produce photons required for photo-neutron reaction.

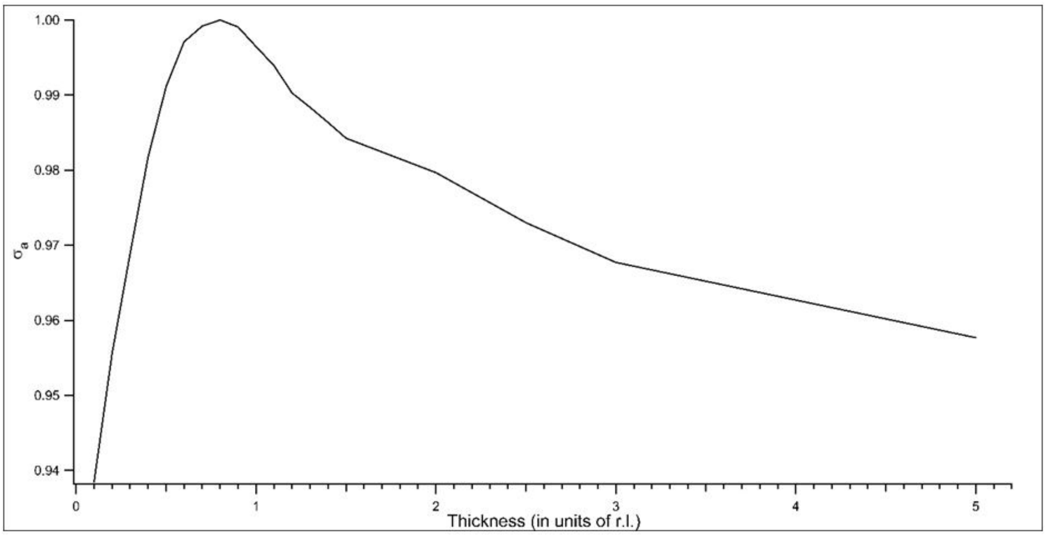

Figure 7: Normalized flux weighted average reaction cross-section (σ_a) for ^{100}Mo(γ,n)^{99}Mo reaction plotted against various thickness of converter target, tungsten

Activity Calculation: Calculation of Activity, A is done using Eq. (2)

$$A = \left(1 - e^{-\lambda t}\right) V I_e \left(\frac{\omega \rho N_a}{M}\right) \int \Phi_{GEANT4}(E)\,\sigma(E)\,dE \quad (2)$$

Where, I_e represents current in units of number of electrons. λ, t, V, ω, ρ, N_a and M are decay constant of ^{99}Mo, irradiation time, volume, mass fraction, density, Avogadro's number and molar mass of ^{100}Mo target, respectively [27]. Integral term is the area under the GDR curve for ^{100}Mo (γ,n) ^{99}Mo reaction and photon flux obtained from GEANT4 (shaded region in Figure 8).

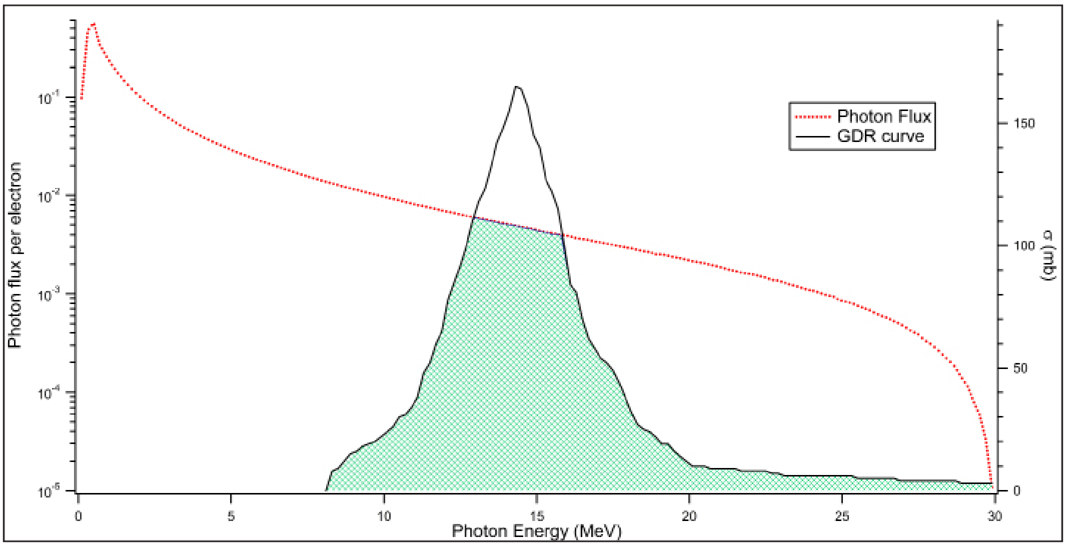

Figure 8: Integrated cross section of photon flux and reaction probability for the ^{100}Mo(γ,n)^{99}Mo reaction

Using the cross-section curve and GEANT4 output, our geometric parameters give activity of 0.951 Ci/mA/day/g (35.18 GBq/mA/day/g) of ^{99}Mo. With 97% enriched Mo activity calculated is 0.923 Ci/mA/day/g (35.151 GBq/mA/day/g). There is very slight change in the activity calculated using 97% enriched Mo. Therefore, depending on the per gram cost of enriched Mo, its design will be fixed. Figure 9 shows change in specific activity with irradiation time.

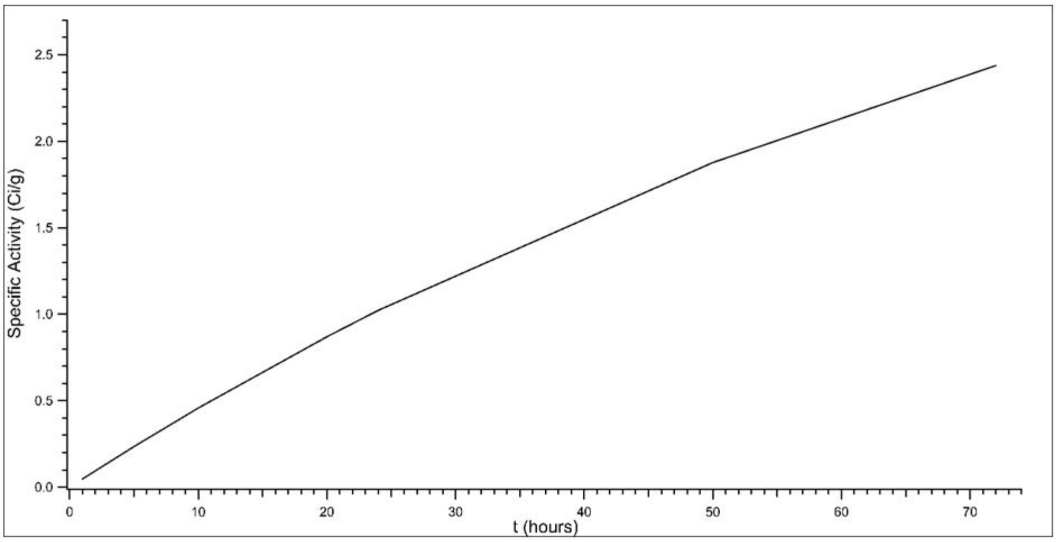

Figure 9: Increase in specific activity with respect to irradiation time from converter target method

Collimation of Photon Flux

In converter target design, ^{100}Mo is kept at some distance from tungsten target. Due to this experimental arrangement the photons coming in forward 30° cone angle will fall on ^{100}Mo. Figure 10 shows the decrease in photon flux intensity when only 30° forward cone angle is used.

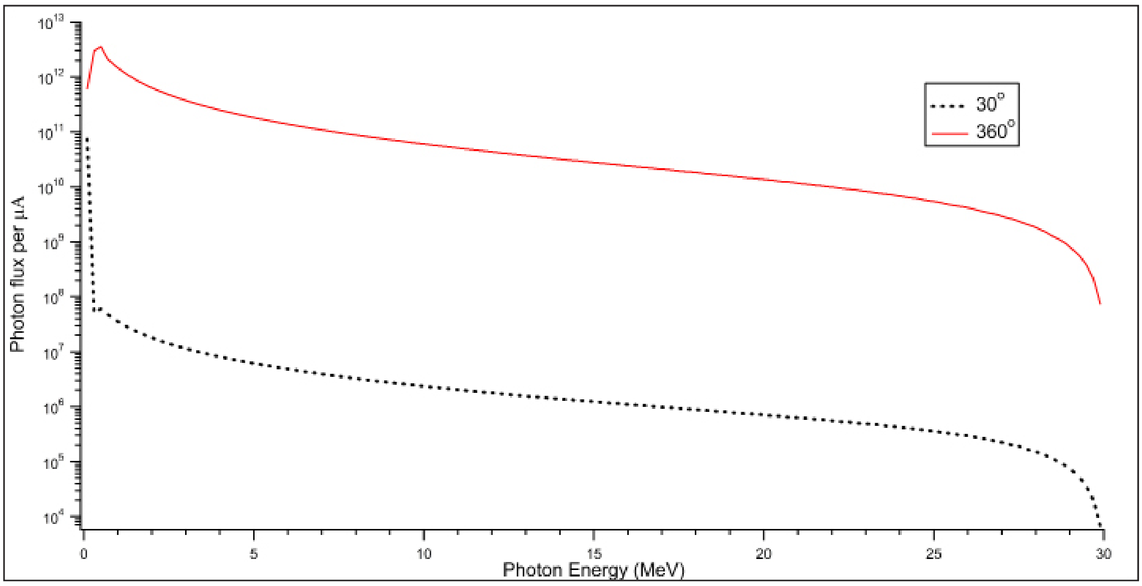

Figure 10: Comparison of reduced photon flux due to collimation in forward 30° angle

This photon collimation reduces specific activity by 55% and it comes down to 0.428 mCi/µA/day/g (15.836 GBq/mA/day/g). But collimation of photon flux is important to reduce residual radioactivity and also to decrease shielding requirements in other directions.

Activity Calculation using Neutron Flux coming out of ^{100}Mo: Photon flux information is used in Eq. (2) to calculate activity of ^{99}Mo, whereas another method of activity calculation uses value of neutron flux from ^{100}Mo. This method gives direct estimate of ^{99}Mo production since number of neutrons coming out of ^{100}Mo are directly proportional to number of photo-neutron reactions taking place. Therefore, an estimate of (γ, xn) reaction taking place inside ^{100}Mo target can be done by counting the neutrons coming out of ^{100}Mo. In converter target method neutron flux is found to increase when ^{100}Mo is added after tungsten. It implies that the photons coming out of tungsten interact with ^{100}Mo and produce photo-neutrons. An apparent increase in neutron flux when ^{100}Mo is added after tungsten is visible in Figure 11.

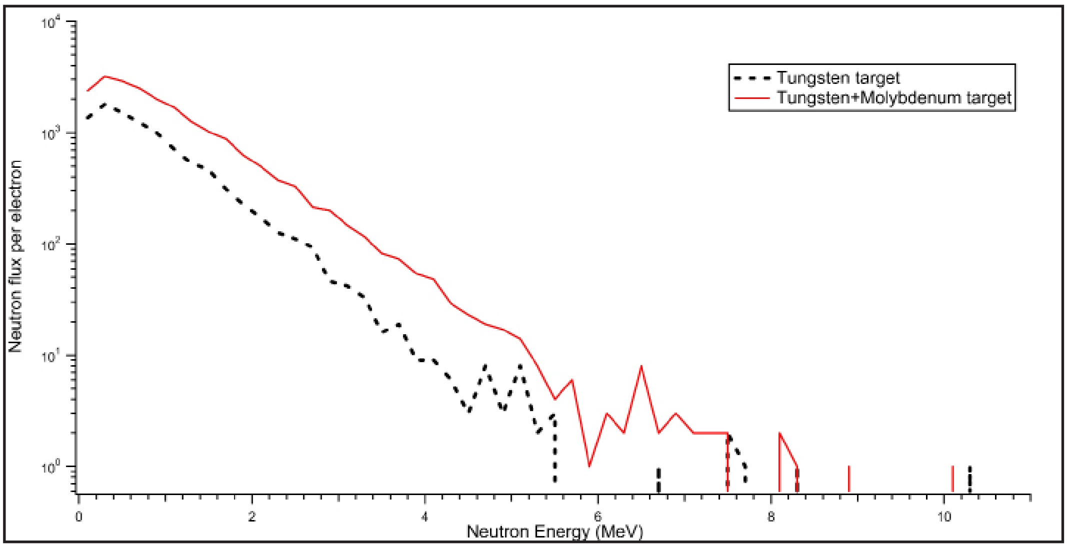

Figure 11: Increase in neutron flux after adding ^{100}Mo target after W converter target

To make precise estimate of neutron flux, an electron beam hitting two targets (^{100}Mo kept after W) and a neutron detector around ^{100}Mo is simulated in GEANT4. A schematic of converter target method with neutron detector is given in Figure 12.

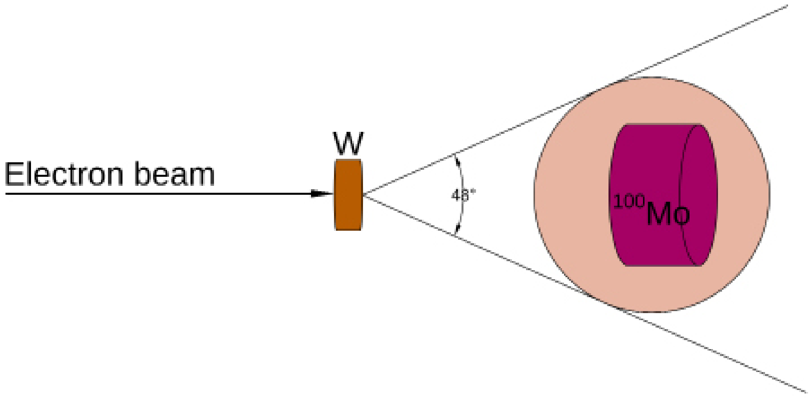

Figure 12: Schematic diagram of converter target and neutron detector assembly and estimation of neutron flux by using GEANT4 simulation

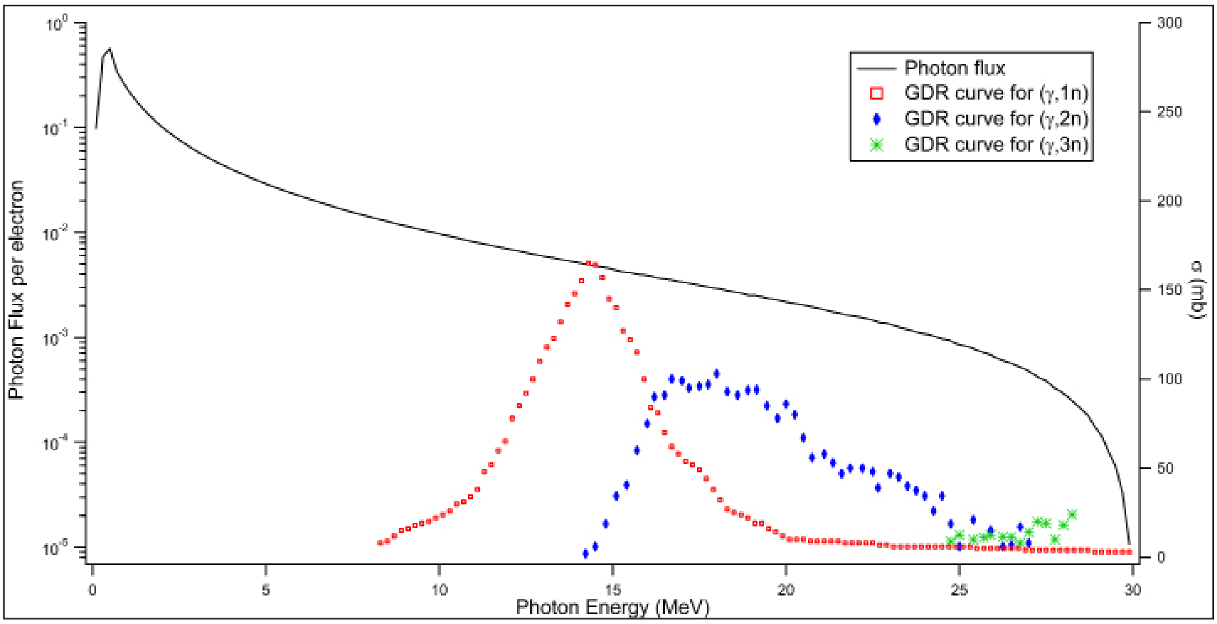

Figure 13: The reaction cross-sections for (γ, n) (γ, 2n) and (γ, 3n) reactions on ^{100}Mo along with the photon flux obtained from tungsten target using GEANT4 simulations

The position of neutron detector is such that it detects the neutrons coming out of ^{100}Mo from all the directions and neutrons coming from tungsten in forward 48 º direction as well. The isotropic nature of neutron flux makes it possible to estimate the flux of neutron coming from tungsten in 48º forward cone angle. This flux is then subtracted from the total neutron flux detected in the neutron detector. By using aforementioned geometric set up shown in fig 12 and isotropic nature of neutron flux distribution, the number of neutrons coming from ^{100}Mo is found to be 3.37×10^{12} for 1mA beam current. This neutron flux is a result of all photo-neutron reactions like (γ, 1n) (γ, 2n) and (γ, 3n) out of which the only relevant reaction for ^{99}Mo production is (γ, 1n). The reaction cross-sections for (γ, 1n) (γ, 2n) and (γ, 3n) reactions alongside the photon flux obtained from tungsten target using GEANT4 simulations is given in Figure 13.

By calculating the area under the GDR curve for three (γ, xn) reactions and photon flux curve, it is found that about 55% of total neutron flux comes from (γ, 1n) whereas the rest of the neutrons come from other (γ, xn) reaction channels [28]. As mentioned in the TRIUMF report the neutrons coming from the (γ, 1n) reaction give direct estimation of the production of ^{99}Mo. Therefore, Activity using neutron flux can be obtained as follows [29].

$$A = 0.55 N_{Mo} \tag{3}$$

where, N_{Mo} is the neutron flux coming out of ^{100}Mo
Using above Equation (3) activity calculated is 0.745 mCi/μA/g (27.565 GBq/mA/g).

Direct Target Approach

Activity Calculation: In direct target approach, the photons for (γ, n) reaction are produced inside ^{100}Mo target and utilized there itself; therefore it is practically impossible to determine exact count of photons produced and their energies in order to calculate the activity with the help of GDR curve and Equation 2. Hence, for direct target approach neutrons flux coming out of ^{100}Mo target is used to estimate the activity. An electron beam of 30 MeV is hit on ^{100}Mo target and neutron flux is found using GEANT4 simulations. Neutron flux is used in Eq. 3 to estimate the photo-neutron reactions leading to the production of ^{99}Mo.

Target Thickness Optimization: Activity calculations for different thicknesses of ^{100}Mo target is done as shown in Figure 14.

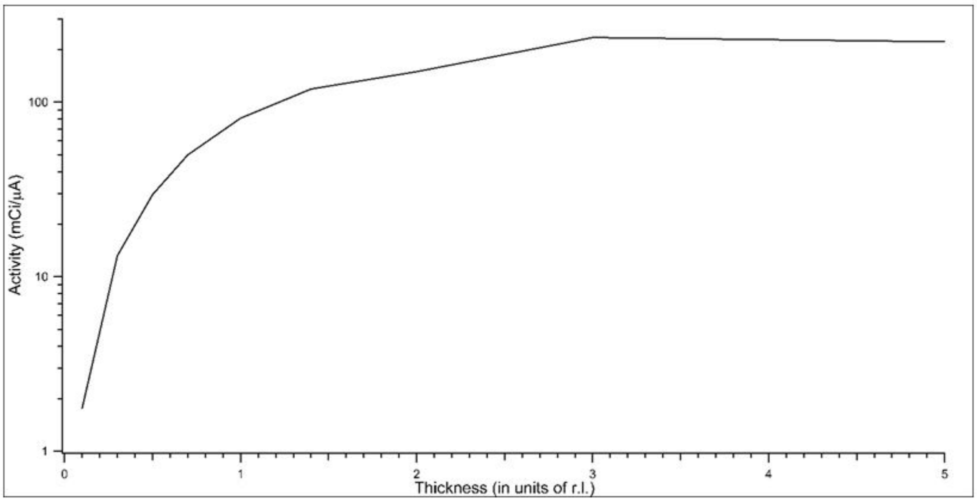

Figure 14: Change in ^{100}Mo activity through direct target method as thickness is increased in the unit of radiation length

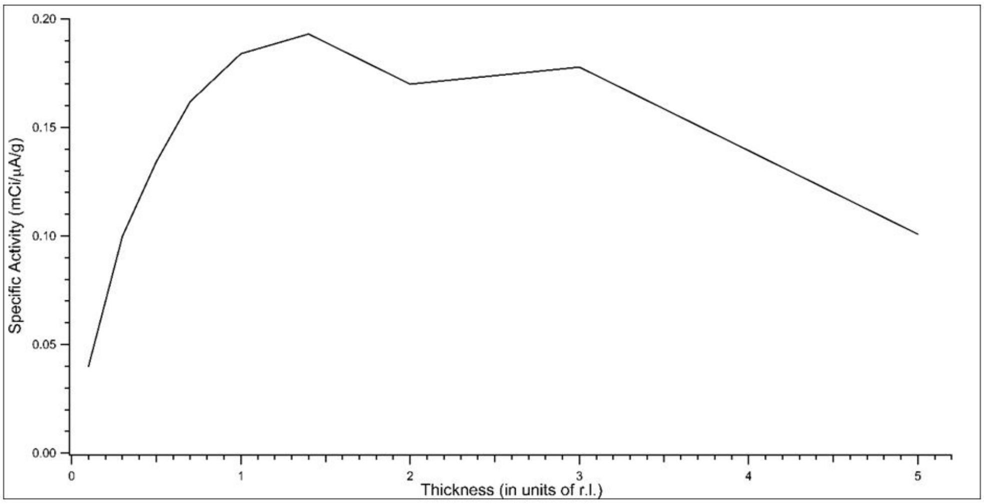

Figure 15: Variation of specific activity of ^{99}Mo as a function of Mo thickness in radiation lengths

It shows that for thicknesses above 1-2 radiation length of Mo target there is no appreciable increase in the activity. ^{100}Mo is an expensive material so increasing its thickness beyond an appreciable length is not cost effective. It can be seen from Figure 15 that increasing ^{100}Mo thickness beyond 1.4 radiation length decreases the overall specific activity. Hence 1.4 r.l. is a reasonable enough thickness for ^{99}Mo production.

Radius Optimization: For comparison of the two approaches viz converter target and direct target, it is important to keep dimension and composition of ^{100}Mo same while calculating activity. In the case of converter target approach, the photons are produced in tungsten and utilized in ^{100}Mo. The geometry and positions of both tungsten and ^{100}Mo is such that if the radius of ^{100}Mo is reduced lesser photons will fall onto it hence reducing the activity. In the case of direct target approach, the photons are produced and utilized in ^{100}Mo itself. Angular distribution of photon flux suggests that most of the photons from 30 MeV electron beam are generated in forward direction. Hence, radius of 12.5 mm is not entirely useful for direct target approach. The radius of cylindrical ^{100}Mo target can be reduced in order to reduce overall mass of ^{100}Mo without drastically affecting the activity. Figure 16 compares the increase in mass of ^{100}Mo and its activity as a function of increasing radius. It can be seen from the plot that above 4 mm of radius (6.88 grams) the increase in activity is not appreciable; suggesting that further increase in radius of ^{100}Mo is not effective in ^{99}Mo production.

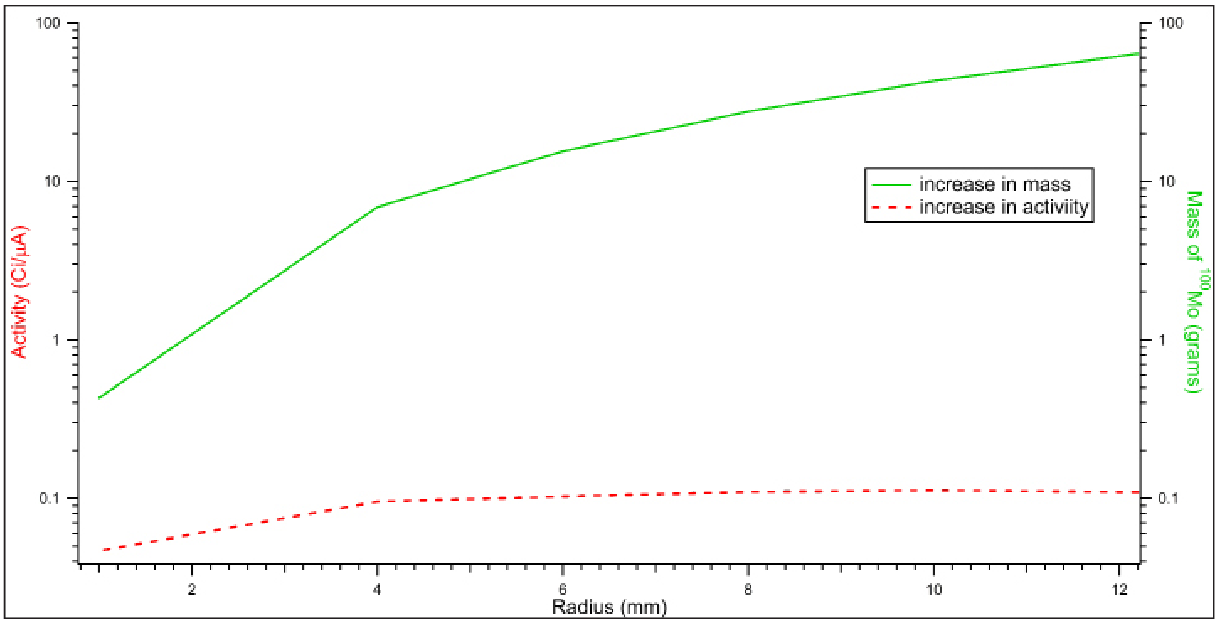

Figure 16: Comparison of increase in mass and activity of ^{100}Mo by varying radius of ^{100}Mo in direct target method

Results

Activity calculation is done using the simulation code GEANT4 and ROOT. For our system namely 30 MeV electron linac with average beam power of 8-10 kW and ^{100}Mo, activity estimate by converter target method is 0.246 Ci/g (9.102 GBq/g) and by direct target method 0.588 Ci/g (21.756 GBq/g) which is based on GEANT4 simulation code. By improvising direct target geometry, it is found that mass specific activity increases more than 7 times. Hence reducing radius of ^{100}Mo target in the case of direct target method gives 4.146 Ci/g (153.402 GBq/g) of activity for 6.88 grams of ^{100}Mo, which is within the suggested range of specific activity by T. Ruth [30].

Discussion

Activity obtained through direct target method and converter target method is compared in Figure 17 to decide more effective way of ^{99}Mo production. The comparison shows that the activity from direct target is consistently more than the activity from converter target method for ^{100}Mo for thickness above 0.2 radiation length. Geometry of direct target approach facilitates production and complete utilization of photons in all 4 π direction, which increases the overall activity, but cooling of Mo target becomes very crucial in this approach. Since, the same target is used for radiochemistry later on therefore; design of mounting of ^{100}Mo for irradiation is very challenging. In converter target method entire beam energy is lost due to absorption in W target therefore cooling mechanism is provided only to W target. For such a high intensity beam a very important parameter is thermal power which could be dissipated on target or converter. Therefore, resolving this cooling problem is a difficult task. Two important factors which needs more consideration are as follows:

a) The target material is usually Mo powder, pressed under very high pressure and melted under micro powder metallurgy. That target material has a very bad thermal conductivity so that the thermal power inside the target is transmitted to target container with low efficiency. So, it needs a special cooling method even using cryogenic methods

b) Decreasing the beam diameter by decreasing the distance between converter (W) and target (^{100}Mo) is a good option for decreasing the mass of target material, but it increases the power density on target. And calculation of optimal distance to compromise the cooling parameters and target material mass is urgently needed.

Lastly, it is observed that for very thin molybdenum targets converter target assembly is more effective, this is because in direct target approach, thin ^{100}Mo target does not stop the electron beam completely. Thus, decreasing the overall available bremsstrahlung photons.

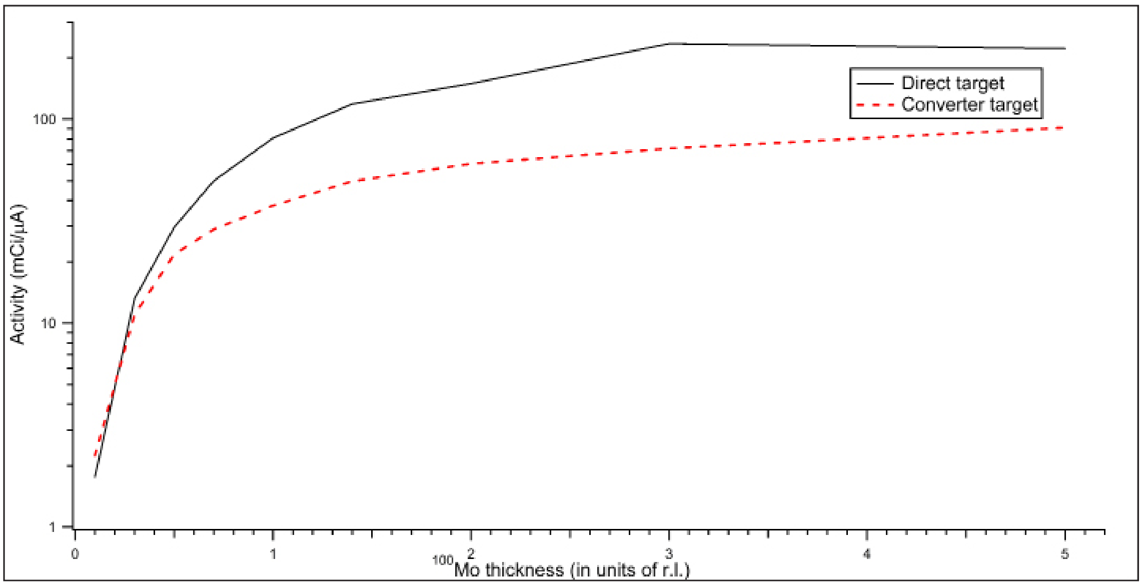

Figure 17: Comparison of ^{99}Mo activity obtained from direct target and converter target method for various thickness of ^{100}Mo

To validate the calculation of activity, data of various references are compared. For converter target method same input parameters as mentioned in the Diamond are used for comparison. Calculations done using Equation 2 and GEANT4 simulation produce activity of 33.16 Ci (1226.92 GBq) for 67.26 grams of ^{100}Mo sample. This is found to be at least 4 times lesser than the activity mentioned by Diamond, *et al.* [18]. In case of direct target method calculations are done for ^{100}Mo of thicknesses 1, 2, and 3r.l. The activities obtained from Equation (3) and GEANT4 simulations for the aforementioned thicknesses are 32.74 Ci/ 26.09 Ci/ 20.12 Ci (1211.38 GBq/965.33 GBq/744.44 GBq), respectively. These values can be compared with the results presented by Tsechanski A [23]. The variation in the activity values is large in most of the references either in converter target method or direct target method. There is no experimental data available to verify the final activity obtained after irradiation. Therefore, a good linac experimental setup to quantify the activity with any beam parameters is important.

Conclusion

It is concluded that for very thin molybdenum targets (~ 0.1 radiation length) converter target assembly is more effective in producing ^{99}Mo via photo neutron reaction, whereas for any thickness beyond 0.1 radiation length direct target method provides much higher specific activity.

Acknowledgment

The author would like to thank Dr. S. V. Suryanarayan and Dr. R. Thomas of Nuclear Physics Division, BARC for their immense help. Author would also like to thank MeitY for supporting the High Energy linac activity for radio-isotope production under grant-in-aid.

References

1. National Nuclear Data Center (2011) NuDat 2.7β, 2011, NNDC, Brookhaven National Laboratory.

2. Harper PV, Lathrop KA, McCardle RJ, Andros G (1964) The Use of Technetium-99m as a Clinical Scanning Agent for Thyroid, Liver and Brain. International Atomic Energy Agency (IAEA) 2: 33-44.

3. Herbert R, Kulke W, Shepherd RT (1965) The use of technetium 99m as a clinical tracer element. Postgrad Med J 41: 656-62.

4. Nuclear Development (2010) The Supply of Medical Radioisotopes, An Economic Study of the Molybdenum-99 Supply Chain. Nuclear Energy Agency 1-126.

5. Daniel Banks (2018) Canada's Neutron Source, The NRU reactor closes. Neutron News 29: 25-31.

6. National Academies of Sciences, Engineering, and Medicine (2016) Molybdenum-99 for Medical Imaging. Committee on State of Molybdenum-99 Production and Utilization and Progress Toward Eliminating Use of Highly Enriched Uranium; Nuclear and Radiation Studies Board, Division on Earth and Life Studies. National Academies Press, US.

7. International Atomic Energy Agency (2010) Technetium-99m Radiopharmaceuticals: Status and Trends. IAEA Radioisotopes and Radiopharmaceuticals Series No 1. IAEA.

8. Loukianova A (2012) What the Doctor Ordered: Eliminating Weapons-Grade Uranium from Medical Isotope Production, NTI.

9. Van der Marck SC, Koning AJ, Charlton KE (2010) The options for the future production of the medical isotope 99Mo. Eur J Nucl Med Mol Imaging 37: 1817-20.

10. Bertsche K (2010) Accelerator Production Option for 99Mo. SLAC-PUB-14132.

11. Nagai Y, Hatsukawa Y (2009) Production of 99Mo for Nuclear Medicine by 100Mo(n,2n)99Mo. J Phys Soc Japan, 78: 1-4.

12. Buono S, Burgio N, Maciocco L (2010) Technical evaluation of an accelerator driven production of Mo-99for Tc-99m generators at CERN (MolyPAN project). Physics for Health, CERN.

13. Ruth T (2009) Accelerating production of medical isotopes. Nature 457: 536-7.

14. Sabel'nikov AV, MaslovL OD, Molokanova G, Gustova MV, Dmitriev SN (2006) Preparation of 99Mo and 99mTc by 100Mo(γ,n) photonuclear reaction on an electron accelerator, MT-25 microtron. Radiochem 48: 191-4.

15. Dikiy NP, Dovbnya AN, Krasnoselsky NV, Lyashko, Yu V, et.al. (2015) The use of molybdenum oxide nanoparticles for production of free isotope Mo-99. Int Nuclear Inf Sys 6: 154-6.

16. Toth JJ, Greenwood LR, Soderquist CZ, Wittman RS, Pierson BD (2011) Production of Molybdenum-99 Using Neutron Capture Methods. United States Department of energy.

17. National Academies of Sciences, Engineering, and Medicine (2018) Opportunities and Approaches for Supplying Molybdenum-99 and Associated Medical Isotopes to Global Markets: Proceedings of a Symposium Washington, DC: The National Academies Press.

18. Diamond W, Nagarakal V, de Jong M, Christopher R, Linda L, et. al. (2014) Production of Molybdenum-99 using electron beams. United States Patent Application Publication, United States.

19. Deshpande A, Dixit T, Urakawa J, Washio, Masakazu, et al. (2011) S-band linac based X-ray source with pi/2 mode electron linac. Nucl Instrum Methods Phys Res Sect A: Accel Spec Detectors Associated Equipment 637: S62-6.

20. Singh S, Dixit T, Deshpande A, Nainwad C (2017) Thermal Estimate of 30 MeV High Energy Linear Accelerator for Radio-Isotope Production, Proceedings of National Conference on Emerging Trends in Vacuum Electronic Devices & Applications, VEDA 2016, Paper No. 045: 1-117.

21. Agostinelli S, Allison J, Amako K, Apostolakis J, Araujo H, et al. (2003) Geant4-a simulation toolkit. Nuclear Instruments and Methods in Physics Research Section A: Accelerators, Spectrometers, Detectors and Associated Equipment. 506: 250-303.

22. Martin JB, Seltzer SM (1970) Bremsstrahlung and Photoneutrons from Thick Tungsten and Tantalum Targets. Phys Rev C2: 621.

23. Tsechanski A, Bielajew AF, Archambault JP, Mainegra-Hing E (2016) Electron accelerator-based production of molybdenum-99: Bremsstrahlung and photo neutron generation from molybdenum vs. tungsten. Nucl Instrum Methods Phys Res Section B: Beam Interactions with Materials and Atoms 366: 124-39.

24. Barber WC, George WD (1959) Neutron Yields from Targets Bombarded by Electrons. Phys Rev J Arch 116: 1551.

25. Beil H, Bergere R, Carlos PA, Lepretre A, De Miniac, et al. (1974) A Study of the photoneutron contribution to the giant dipole resonance in doubly even Mo isotopes. Nucl Physics A 227: 427-49.

26. Naik H, Suryanarayana SV, Jagadeesan KC, Thakare SV, Joshi PV, et al. (2012) An alternative route for the preparation of the medical isotope 99Mo from the 238U(γ, f) and 100Mo(γ, n) reactions. J Radioanal Nucl Chem 295: 807-16.

27. Jang J, Yamamoto M, Uesaka M (2017) Design of an X-band electron linear accelerator dedicated to decentralized 99Mo/99mTc supply: From beam energy selection to yield estimation. Phys Rev Accel Beams 20: 104701.

28. Young-Ouk L, Chang J, Kim, Doohwan K, Lee JY et.al. (2002) High Energy Nuclear Data Evaluations for Neutron-, Proton-, and Photon-induced Reaction Data at KAERI. J Nuclear Sci Technol 39: 60-3.

29. TRIUMF (2008) Report of the Task Force on Alternatives for Medical Isotope Production. TRIUMF.

30. Thomas R (2014) The Medical Isotope Crisis: How We Got Here and Where We Are Going. J Nucl Med Technol 42: 245-8.